Electronic Supplementary Information

Investigating Acid-Induced Structural Transitions of Lysozyme in an Electrospray Ionization Source

Jong Wha Lee[a] *and Hugh I. Kim*[a,b,*]

[a]Department of Chemistry, and [b]Division of Advanced Materials Science, Pohang University of Science and Technology (POSTECH), Pohang, 790-784, South Korea

[*]To whom correspondence should be addressed: E-mail: hughkim@postech.edu

Table of contents

Supporting Methods

Computational Modeling. GROMACS 4.5.5[1] and all-atom OPLS force field[2] were used for all simulations. Velocity rescaling thermostat[3] was used to control the temperature with a coupling constant of 0.1 ps. LINCS[4] was used to constrain the bonds, and a time step of 2 fs was used for solution-phase simulations and 1 fs for gas-phase simulations. The cut-offs were removed for gas-phase simulations. The Ω_D values were calculated with EHSS[5] and TJ[6] model. As the TJ model requires too high computational cost, we majorly use EHSS model throughout the paper, and compare the values from TJ model. The differences in the resulting values from two models were small.

For molecular modeling of Lyz in solution with SAXS curves, crystal structure of Lyz (PDB code: 2LYZ)[7] was subjected to various annealing protocols including constant temperature simulations at 350 K, 400 K, 500 K, 600 K, 700 K, 800 K, 900 K, or 1000 K, and periodic annealing simulations from 300 K to 400 K, 500 K, 600 K, 700 K, 800 K, 900 K, or 1000 K. The simulations were performed in implicit solvent[8, 9] for efficient conformation search. α-helix and β-sheet secondary structures were maintained with distance restraints to facilitate the search as Lyz in aqueous solutions exhibited very similar CD ellipticities (Figure S1). Over 200,000 conformations were generated with the process. Theoretical scattering curve of each structure was generated and compared with experimental scattering curves of Lyz with CRYSOL program.[10] Candidate solution structure of Lyz was selected from conformations with R_g value within ±1 Å of the experimental value, with small discrepancy value (χ) from experimental SAXS curve, and with secondary structure contents similar to that of the native Lyz.

For gas-phase simulations, we used charge configurations that gives the lowest energy in terms of electrostatic interactions. This is because protein charging is believed to occur at late stages of ESI and follow gas-phase energetics,[11] and electrostatic interactions are dominant in the gas phase. As Coulomb potential is inversely proportional to the distance between two point charges, the inverse of the distances

were summed up to evaluate relative Coulomb energies between all possible charge configurations for a given charge state of Lyz (eq. S1).

$$\sum_i \sum_j \frac{q_i q_j}{r_{ij}} \ (i \neq j) \quad \text{(S1)}$$

i and *j* represent all the basic and acidic residues in Lyz. It is possible that the charge site configurations used in the present study does not fully represent the actual charge configuration of Lyz after ESI. It is possible that solution-phase salt-bridges are maintained after ESI. Moreover, protons may not be localized at a single site. However, we believe our charge site configuration could be a representative configuration. This simple model innately considers retaining of salt-bridges favorably, and protons are expected to favor configurations with low-energy even if they are mobile.

Before all simulations, Lyz was subjected to steepest descent minimization. For constant temperature simulation, Lyz was heated from 0 K to 300 K in 100 ps and simulated at 300 K for 29.9 ns. For simulated annealing, Lyz was heated to 1000 K for 0.2 ns, maintained at the temperature for the next 0.8 ns, cooled to 300 K for 0.5 ns, and the temperature was maintained for the next 1 ns. This protocol was repeated for 100 cycles. Fluctuations in root-mean-square deviations were small after 1 ns of equilibration at 300 K.

Previous simulation study of Lyz by Tapia and co-workers reported that thermally unfolded Lyz refolds with rich secondary structural contents.[12] However, our simulations using different force fields (OPLS[2] and GROMOS53a6[13]), different annealing temperatures (500 K and 1000 K), thermostat (Berendsen[14] and velocity rescaling[3]), different annealing time (total 2.5 ns/cycle and 6 ns/cycle) and charge site configurations did not yield Lyz with rich secondary structures. Even short annealing at 500 K diminished most secondary structures of Lyz and which were not reformed by equilibration after cooling to 300 K. This discrepancy may be due to different charge site configuration assignment. We have chosen the charge site configurations based on scores on a model considering relative energies in the gas phase and taken into account the presence of

negative charges. However, the previous simulation study has distributed the net charge equally into all basic sites.[12]

Figure S1. Experimental SAXS curves, theoretical fit to the experimental curves, and discrepancy value (χ) for a) models in Figure 1e, and b) models in Figure 1f. in the main text.

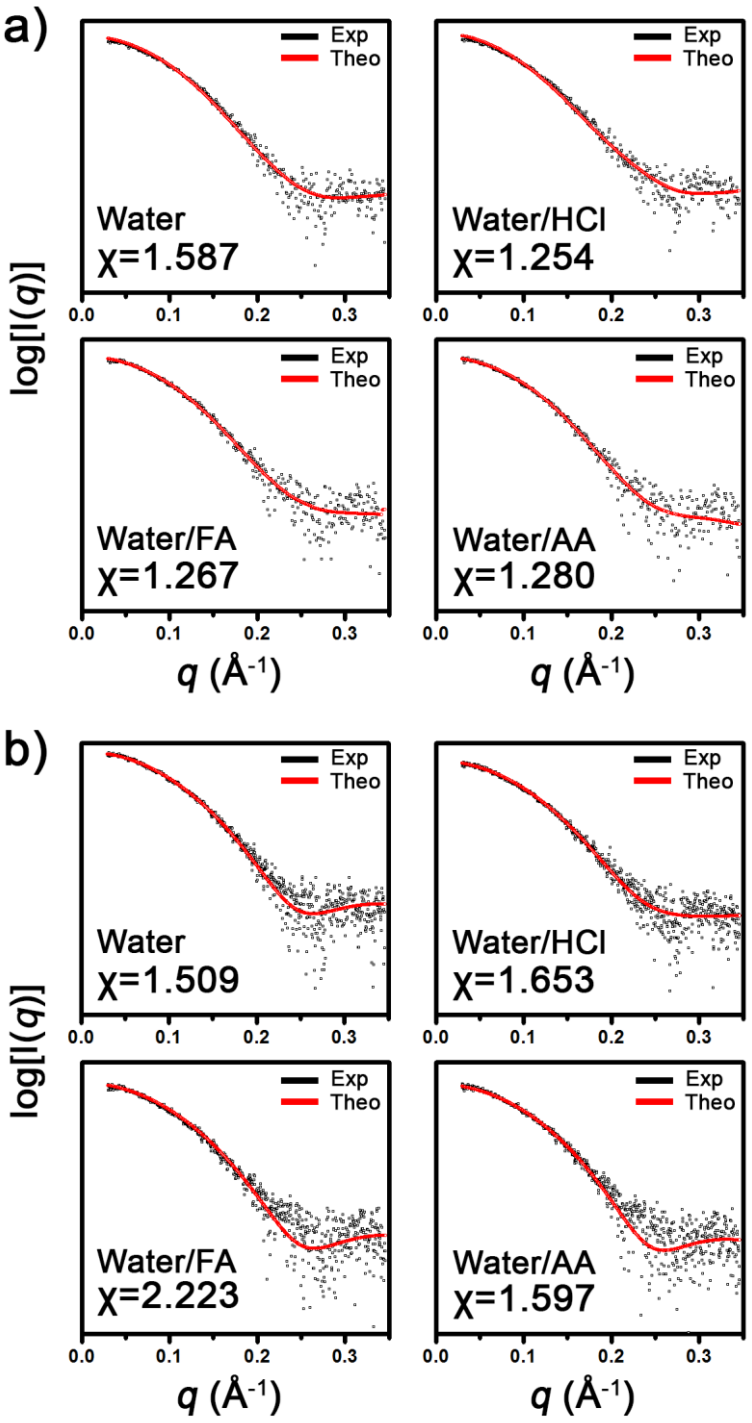

Figure S2. Additional candidate molecular models of Lyz.

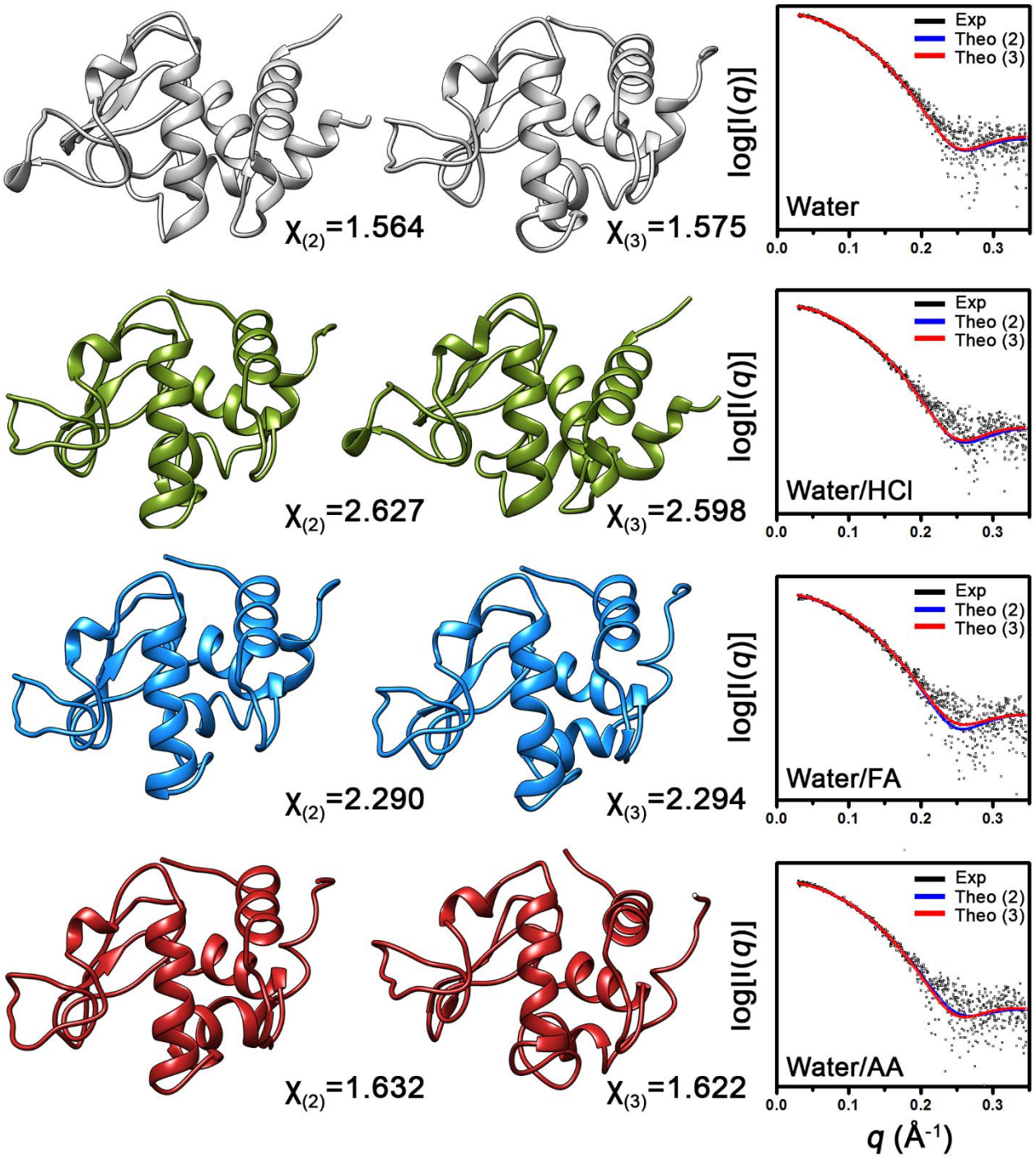

Figure S3. Secondary structure analyses of molecular models of Lyz in Figure S2 with STRIDE.

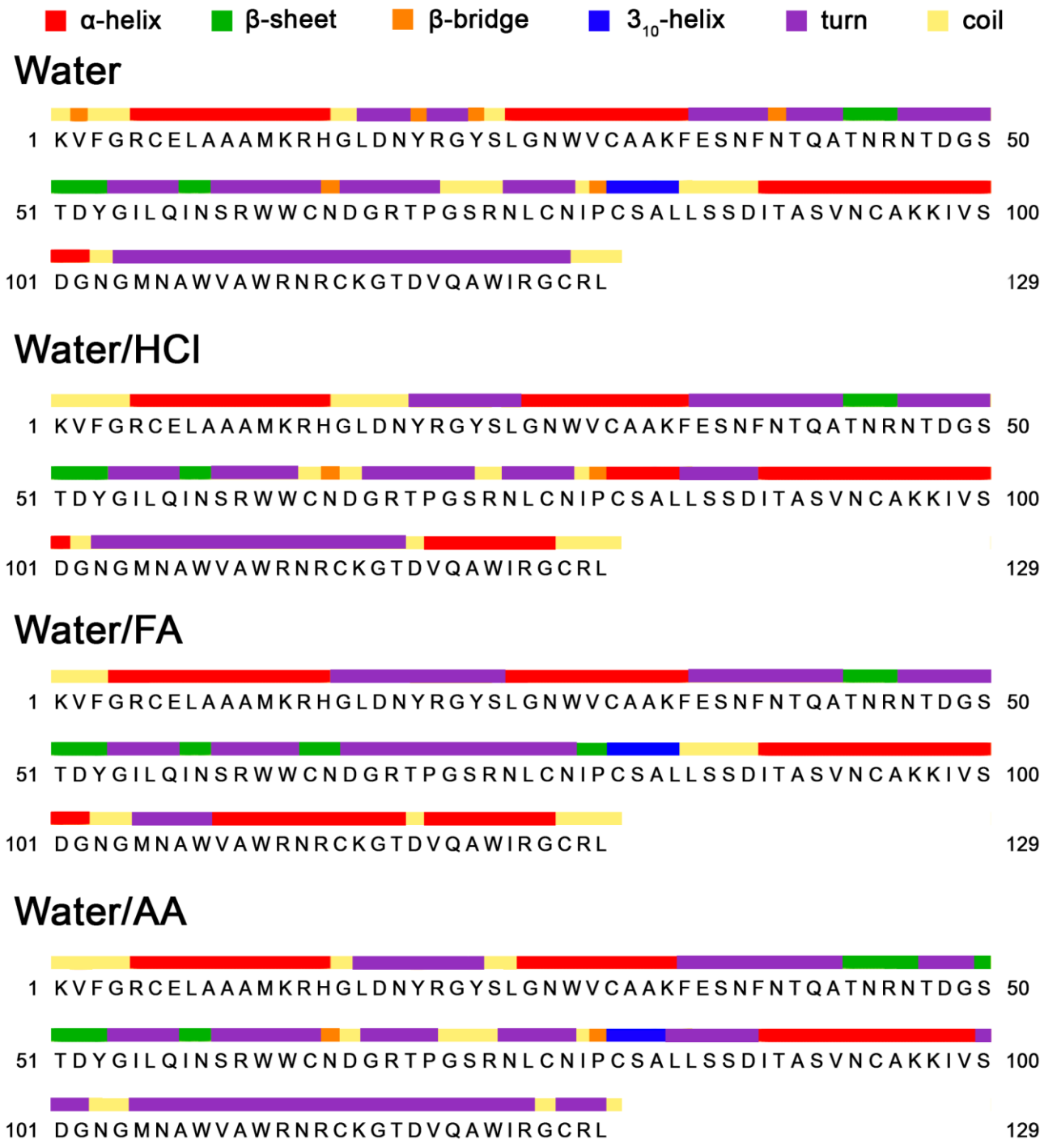

Figure S4. a) ESI-MS spectrum and b) IM spectra of Lyz at +6, +7, +8, and +9 charge states, in 50 mM ammonium acetate solution (pH 7).

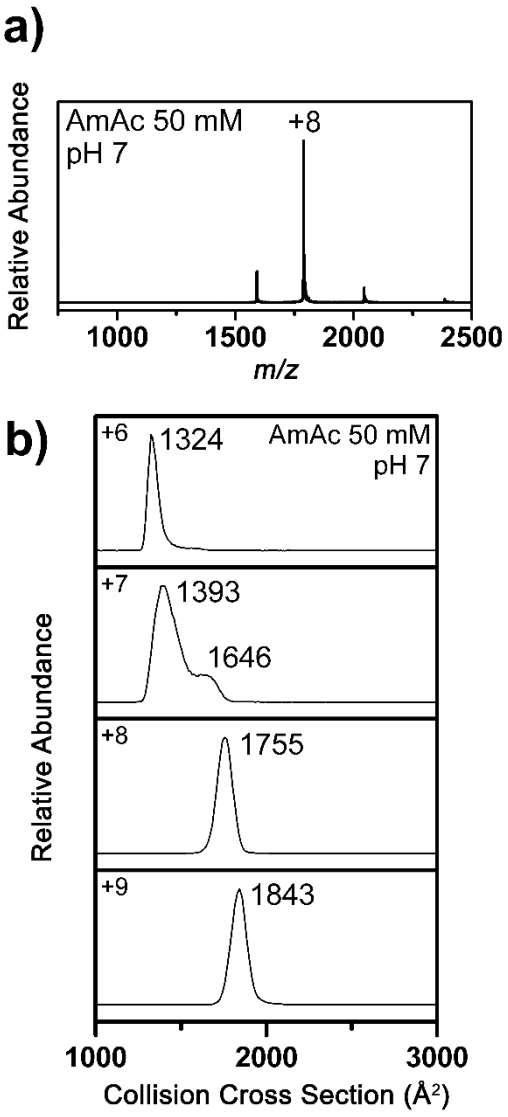

Figure S5. ESI-MS spectra of Lyz from aqueous solution with 0.1% v/v FA at pH 2.7, and 0.1% v/v FA with HCl at pH 2.2

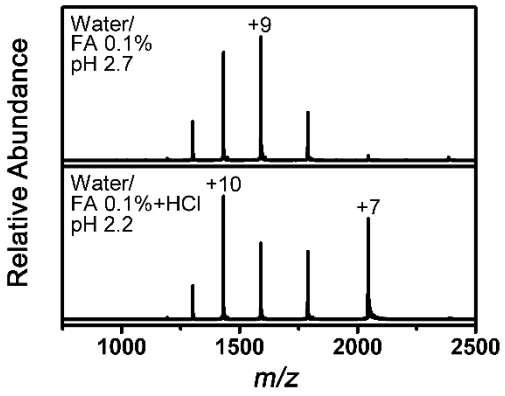

Figure S6. Time-dependent Ω_D profiles for +6 and +7 charged Lyz in the gas phase at 300 K. The Ω_D values are calculated with the EHSS model. The average values and errors are the average and standard deviation from last 20-ns trajectories of the simulations.

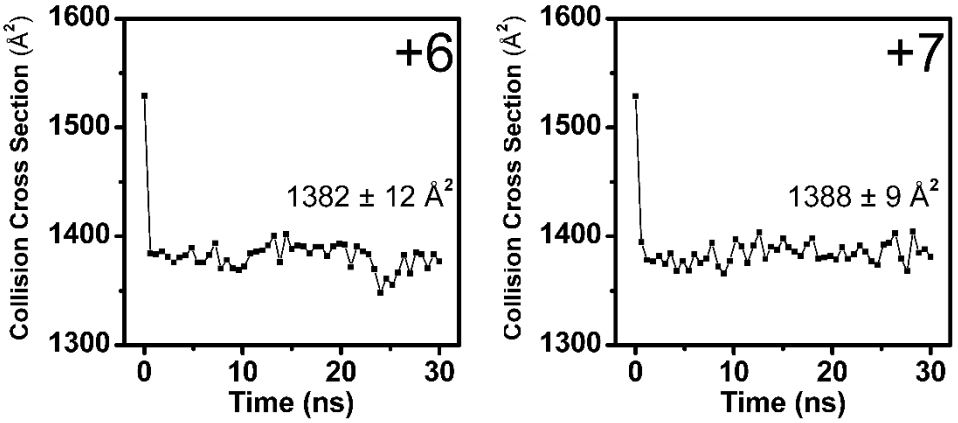

Figure S7. Scatter plot of potential energy versus Ω_D for Lyz ions from simulated annealing simulations.

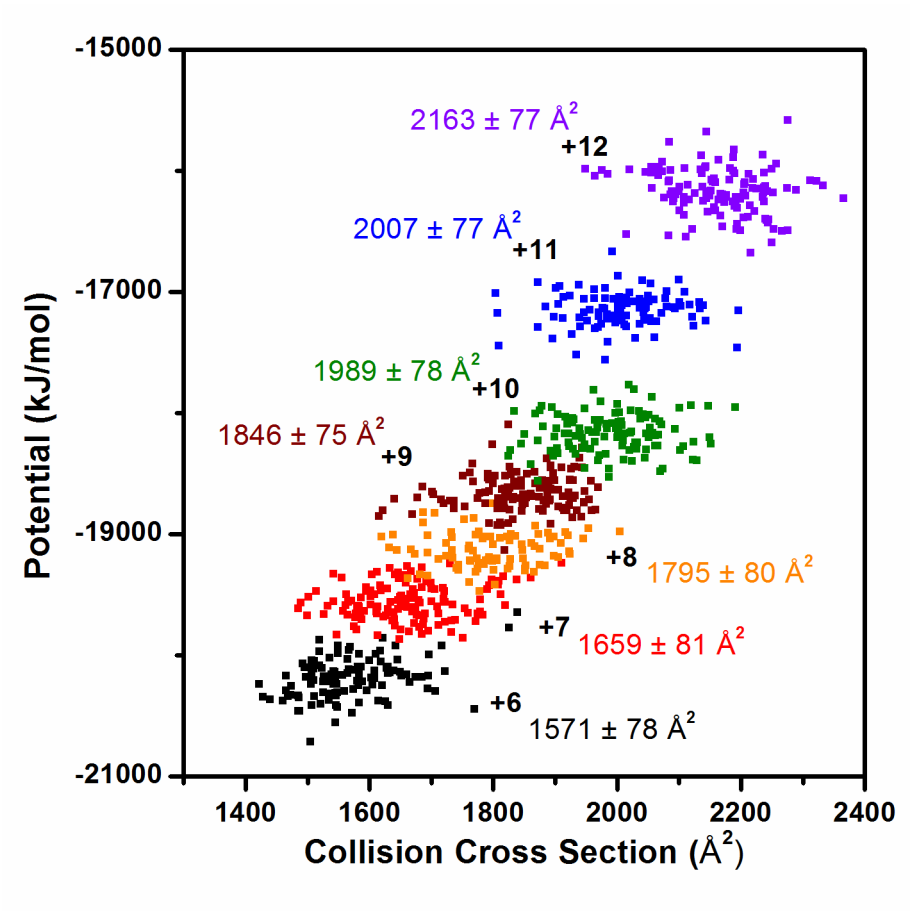

Figure S8. Representative structure of +8 to +11 charged Lyz ions from simulated annealing. Ω_D values from both the EHSS and the TJ model are given as insets.

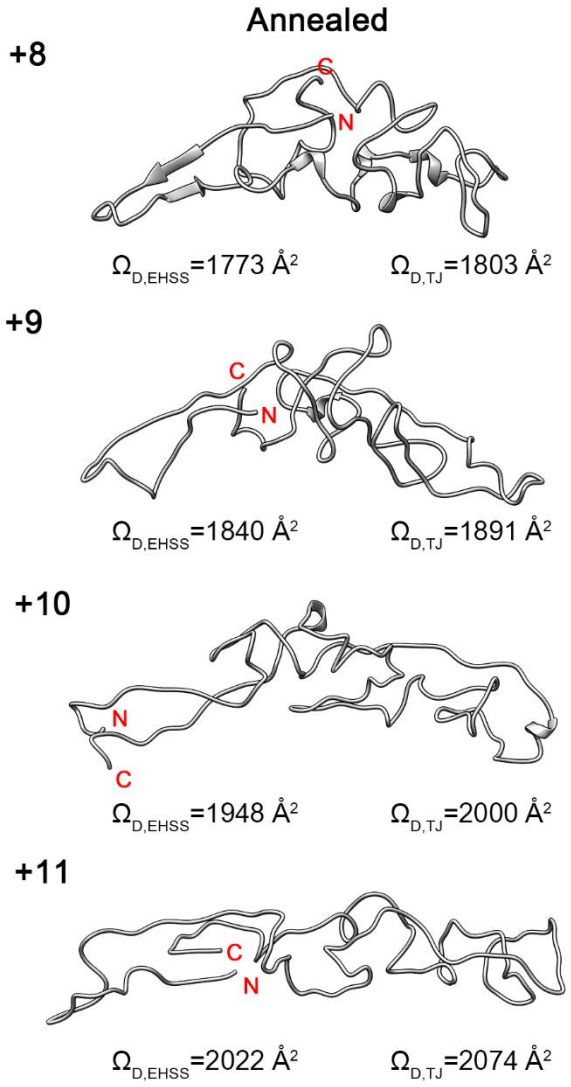

Table S1. Comparison between Ω_D values (Å^2) of Lyz from water solution in this work and those from drift-tube IM experiments. The values are from either Clemmer group homepage (http://www.indiana.edu/~clemmer/), or from Figure 7 in their work.[15]

Charge state	This work	Drift-Tube
+6	1342	1355
+7	1382, 1491, 1666	1364, ~1480, 1674, 2057
+8	1787	1363, 1781, 2203
+9	1843	1407, 1899, 2384
+10	1913	1446, 1961, 2390
+11	2025	~2000
+12	2102	-

Table S2. Comparison between experimental Ω_D values of B class Lyz ions from aqueous FA solution and average theoretical Ω_D values of simulated structures from EHSS model. Errors in the experimental and theoretical values are full-width-half-maximum values and one standard deviations of all Ω_D values, respectively.

Charge state	**Experimental** Ω_D (Å^2)	**Theoretical** Ω_D (Å^2)
+6	1482 ± 143	1571 ± 78
+7	1654 ± 112	1659 ± 81
+8	1770 ± 107	1795 ± 80
+9	1838 ± 119	1846 ± 75
+10	1944 ± 110	1989 ± 78
+11	2046 ± 103	2007 ± 77
+12	2183 ± 83	2163 ± 77

References

1. B. Hess, C. Kutzner, D. van der Spoel and E. Lindahl, *J. Chem. Theo. Comput.*, 2008, **4**, 435-447.
2. G. A. Kaminski, R. A. Friesner, J. Tirado-Rives and W. L. Jorgensen, *J. Phys. Chem. B*, 2001, **105**, 6474-6487.
3. G. Bussi, D. Donadio and M. Parrinello, *J. Chem. Phys.,* 2007, **126**, -.
4. B. Hess, H. Bekker, H. J. C. Berendsen and J. Fraaije, *J. Comput. Chem.*, 1997, **18**, 1463-1472.
5. A. A. Shvartsburg and M. F. Jarrold, *Chem. Phys. Lett.*, 1996, **261**, 86-91.
6. M. F. Mesleh, J. M. Hunter, A. A. Shvartsburg, G. C. Schatz and M. F. Jarrold, *J. Phys. Chem.*, 1996, **100**, 16082-16086.
7. R. Diamond, *J. Mol. Biol.*, 1974, **82**, 371-391.
8. M. Schaefer, C. Bartels and M. Karplus, *J. Mol. Biol.*, 1998, **284**, 835-848.
9. A. Onufriev, D. Bashford and D. A. Case, *Proteins: Struct., Funct., Bioinf.*, 2004, **55**, 383-394.
10. D. Svergun, C. Barberato and M. H. J. Koch, *J. Appl. Crystallogr.*, 1995, **28**, 768-773.
11. M. I. Catalina, R. H. H. van den Heuvel, E. van Duijn and A. J. R. Heck, *Chem. Eur. J.*, 2005, **11**, 960-968.
12. C. T. Reimann, I. Velázquez, M. Bittner and O. Tapia, *Phys. Rev. E*, 1999, **60**, 7277-7284.
13. C. Oostenbrink, A. Villa, A. E. Mark and W. F. Van Gunsteren, *J. Comput. Chem.*, 2004, **25**, 1656-1676.
14. H. J. C. Berendsen, J. P. M. Postma, W. F. v. Gunsteren, A. DiNola and J. R. Haak, *J. Chem. Phys.*, 1984, **81**, 3684-3690.
15. S. J. Valentine, J. G. Anderson, A. D. Ellington and D. E. Clemmer, *J. Phys. Chem. B*, 1997, **101**, 3891-3900.